Journal of ELECTRONIC MATERIALS, Vol. 48, No. 4, 2019
https://doi.org/10.1007/s11664-019-06974-5

TOPICAL COLLECTION: INTERNATIONAL CONFERENCE ON THERMOELECTRICS 2018

The Importance of Considering Parasitic Heat Losses When Modeling TEG Performance for High-Temperature Applications

R. SCHWURACK,[1,2] S. UNZ,[1] and M. BECKMANN[1]

1.—Institut für Verfahrenstechnik und Umwelttechnik, Technische Universität Dresden, George-Bähr-Straße 3b, 01062 Dresden, Germany. 2.—e-mail: roy.schwurack@tu-dresden.de

For a thermoelectric generator (TEG) with nonideal heat exchangers, the electrical power output can be maximized by matching the thermal resistances of the TEG R_{teg} and heat exchangers R_{hx}. Due to the fact that TEG elements are not thermally isolated from the surroundings, this study shows that inner heat losses are significant for proper thermal resistance matching—particularly for TEG systems for high-temperature applications. The inner heat losses are here defined as parasitic heat transfer mechanisms within the space between the thermoelectric (TE) couple legs. Analytical modeling is carried out using a thermal resistance network and applied to determine the performance of a TE system comprising a finned heat sink as well as a TEG with base area of $A = 6 \times 6 \times 10^{-4}$ m^2 and leg width of $a = 3 \times 10^{-3}$ m. The performance of different TEG designs is evaluated, and the optimum thermal resistance ratio, i.e., R_{hx}/R_{teg}, obtained for different values of leg length and built-in TE couple leg number. Finally, the developed analytical model is employed in a multiobjective TEG design optimization scheme, based on the theory of Pareto efficiency, to maximize the power output while minimizing the amount of TE material required. The results obtained from the multiobjective optimization reveal that the amount of TE material required in a module can be reduced by 6.63% without any power output loss in comparison with the results of one-parameter optimization.

Key words: Thermoelectric generator, heat exchanger, heat loss, high temperature, design optimization, Pareto frontier

INTRODUCTION

Thermoelectric generators (TEGs), i.e., systems which can convert heat directly into electricity, require no moving components and benefit from zero noise emission and no maintenance effort in operation. However, their low efficiency compared with other technologies for use of waste heat (organic Rankine cycle, Stirling engine, etc.), high manufacturing costs, and yet to be proved reliability in harsh environments still prevent large-scale applications to exploit waste heat for effectively improving the efficiency of industrial or automotive facilities. However, TEGs have shown great potential to supply wireless autarkic sensor systems and microcontrollers for monitoring tasks.[1–4]

Thermoelectric systems applied for harvesting waste heat basically consist of a thermoelectric module, heat exchangers linking the thermoelectric module to the heat reservoirs, as well as an electronic module, which is necessary to convert the voltage generated by the thermoelectric module to a regulated voltage level that can be used to supply any electric load. Recent scientific efforts have resulted in major advances in the characterization and performance of thermoelectric materials, leading to an increase in the theoretically achievable maximum power output provided by thermoelectric modules.[5] However, this potential can only be fully exploited for ideal connections to

(Received August 20, 2018; accepted January 16, 2019; published online January 31, 2019)

the heat reservoirs. For real systems with dissipative heat exchangers, the thermoelectric device must be thermally optimized to guarantee the best performance with maximum power output.

An early work by Henderson[6] dealt with this issue, concluding that the best performance can be achieved by adjusting the thermal resistance of the thermoelectric module to the thermal resistance of the heat exchangers. Here, the optimum ratio of the sum of all external thermal resistances (representing the heat exchangers and all contact resistances) to the thermal resistance of the thermoelectric module R_{hx}/R_{teg} is proposed to be equal to 1. This finding was supported later in another investigation on optimization of thermoelectric systems operating on small temperature differences.[7] By simultaneously considering thermal and electrical resistance matching, Apertet[8] defined a condition in relation to the figure of merit ZT with $R_{hx}/R_{teg} = \sqrt{ZT+1}$. Although all these mentioned studies consider dissipative effects due to finite thermal contacts, they neglect parasitic heat losses within the space between the thermoelectric (TE) couple legs.

Internal parasitic heat losses are caused by conduction, convection, and radiation in the space between the thermoelectric legs and the side walls of the TEG. While heat losses to the ambient can partly be reduced by proper insulation, parasitic heat bypass within the TEG can hardly be prevented, hence leading to a decrease in the electrical power output.[9–12] For low temperature ranges and small temperature gradients, this effect is minimal, making it negligible in TEG design optimization studies. In contrast, this work is part of a research activity that aims to develop and manufacture ceramic-based thermoelectric modules for high-temperature applications. Development of new materials that operate effectively at high temperatures allows application of TEGs in high-temperature processes (iron production and chemical industry) and facilities (furnaces, burners, and turbines) and is furthermore seen as a possibility to increase the power output of thermoelectric systems.

The present study deals with design optimization of a TEG–heat exchanger system for application at high temperatures with consideration of temperature-dependent material parameters as well as internal parasitic heat losses. The design strategy relies on the thermal resistance matching according to Ref. 6, with the aim of guaranteeing the maximum power output. To adjust the thermal resistance of the thermoelectric module with a certain fixed base area, the number of thermoelectric legs is identified as a key parameter. The main target is to investigate whether the proposed thermal resistance ratio is also applicable for the targeted conditions. Therefore, an analytical investigation based on a thermal resistance network was carried out.

ANALYSIS

Thermal Resistance Network

The behavior of the TEG system was analyzed based on the model shown in Fig. 1. The investigated thermoelectric module is characterized by a constant base area $A = 6 \times 6 \times 10^{-4}\ \mathrm{m}^2$ and leg width $a = 3 \times 10^{-3}$ m with variable leg length l_l and number of built-in legs n or pairs of thermoelectric n-type and p-type semiconductor legs m, respectively. For a leg length l_l and leg width a, a characteristic leg form factor is defined as $f = l_l/a$, which represents an aggregated dimensionless form to describe the leg geometrical properties that influence the TEG performance. On the cold side, a finned heat sink is applied with $i = 10$ fins having a length of $l_f = 0.1$ m, thickness of $b_f = 2 \times 10^{-3}$ m, and height of $h_f = 6 \times 10^{-2}$ m, equal to the edge length of the thermoelectric module. The base plate is considered to have thickness of $t_f = 5 \times 10^{-3}$ m. Additionally, in this study, the substrate plates and electrical conductors are considered to have equal thickness of $t_{con} = 1 \times 10^{-3}$ m. For titanium oxide (TiO_x) as the n-type thermoelectric semiconductor, boron carbide (B_nC) as the p-type thermoelectric semiconductor, aluminium nitride (AlN) as the substrate material, and copper (Cu) as the electrical conductor, the polynomial constants for calculating the temperature-dependent material data are presented in Tables I and II. For the electrical conductivity (σ) and thermal conductivity (λ) in Table I, $y(T) = \sum_{i=0}^{8} a_i T^i$ applies, while for the Seebeck coefficient (S) in Table II, $y(T) = \sum_{i=0}^{5} a_i T^i / \sum_{b=0}^{4} b_i T^i$ applies, where T is the absolute temperature in Kelvin. With the given polynomials, the material properties are evaluated at an average temperature $\bar{T}$.

For each component of the system, a thermal resistance can be defined, yielding in total a thermal resistance network that must be solved to determine the temperature distribution and TEG performance characteristics. The combined thermal resistance of the substrate plates and electrical conductors R_{con} is given by

$$R_{con} = \frac{t_{con}}{\lambda_{AlN} A} + \frac{t_{con}}{\lambda_{Cu} A}. \quad (1)$$

The parallel interconnection of the thermal resistances of the n- and p-type legs (R_n, R_p) yields the total thermal resistance of the thermoelectric module R_{teg}. Here, the parasitic heat bypass between the legs is additionally considered. Within the gap, heat is assumed to be solely transferred by conduction ($R_{by,\lambda}$) and radiation ($R_{by,\epsilon}$). Convection is neglected, as the air is assumed to be motionless. This assumption is based on the evaluation of the Rayleigh number for the given thermoelectric module configuration.[11] As the Rayleigh number was found to be below a critical value of 1707, heat is primarily transferred by conduction. Heat transfer

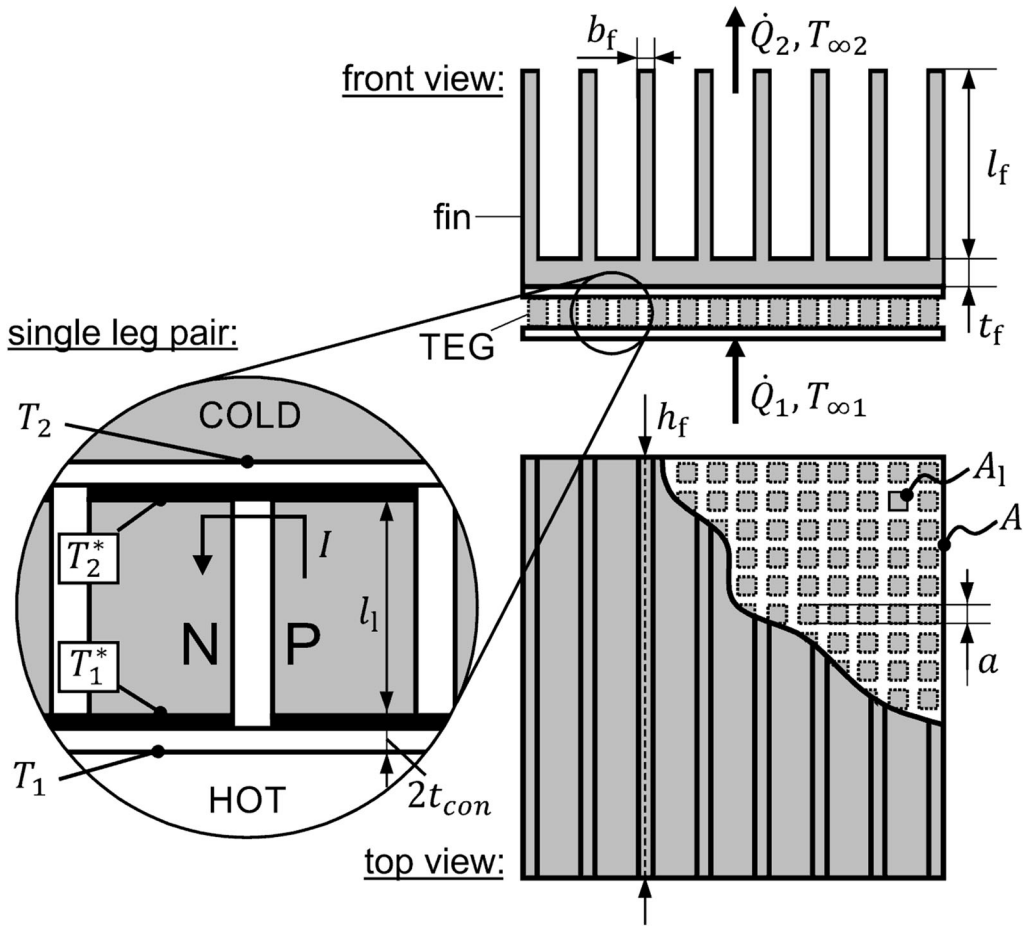

Fig. 1. Schematic of investigated TEG–heat exchanger system.

from the leg side walls is not considered, since the temperature field in the plane parallel to the substrate plates is assumed to be uniform. In sum, this yields

$$R_{\text{teg}} = \left[\frac{1}{R_n} + \frac{1}{R_p} + \frac{1}{R_{\text{by},\lambda}} + \frac{1}{R_{\text{by},\epsilon}}\right]^{-1} \tag{2}$$

with $R_n = l_l/(\lambda_{\text{TiO}} m a^2)$, $R_p = l_l/(\lambda_{\text{BC}} m a^2)$, $R_{\text{by},\lambda} = l_l/(\lambda_{\text{Air}}(A - n a^2))$, and $R_{\text{by},\epsilon} = 1/(\alpha_\epsilon (A - n a^2))$ with n as the number of built-in legs and m as the number of pairs of thermoelectric n-type and p-type semiconductor legs. The effective heat transfer coefficient for radiation α_ϵ is not a plain material parameter, but has to be calculated by

$$\alpha_\epsilon = \epsilon_{\text{res}} \sigma_{\text{SB}} \frac{(T_1^{*4} - T_2^{*4})}{T_1^* - T_2^*}, \tag{3}$$

where $\sigma_{\text{SB}} = 5.67 \times 10^{-8}\ \text{W/m}^2/\text{K}^4$ is the Stefan–Boltzmann constant. For the resulting emission coefficient ϵ_{res} within the TEG, extensive analysis can be found in Ref. 13. In this study, a simple analytical approach using two infinite parallel plates with $\epsilon_{\text{res}} = 1/(2\epsilon^{-1} - 1)$ is applied. The material-specific emission coefficient is assumed to be $\epsilon = 0.9$.

The thermal resistance of the heat exchanger, in turn, can be defined as

$$R_{\text{hx}} = \frac{1}{\alpha(\eta_f A_{f1} + A_{f2})} + \frac{t_f}{\lambda_{\text{Cu}} A} \tag{4}$$

with the heat transfer coefficient α determined by proper Nusselt functions,[14] the overall surface of all fins $A_{f1} = 2 i l_f (b_f + h_f)$, the unfinned surface $A_{f2} = A - i b_f h_f$, and the fin efficiency rate $\eta_f = \tan h(\mu l_f)/(\mu l_f)$ with $\mu = [2\alpha(b_f + h_f)/(b_f h_f \lambda_{\text{Cu}}]^{1/2}$, according to Ref. 15.

By applying the defined thermal resistances, the incoming and outgoing heat fluxes are determined as

$$\dot{Q}_1 = \frac{1}{R_{\text{hx1}}}(T_{\infty 1} - T_1) = \frac{1}{R_{\text{con}}}(T_1 - T_1^*), \tag{5}$$

$$\dot{Q}_2 = \frac{1}{R_{\text{hx2}}}(T_2 - T_{\infty 2}) = \frac{1}{R_{\text{con}}}(T_2^* - T_2). \tag{6}$$

Table I. Polynomial constants for calculating the electrical and thermal conductivity for the applied materials

	Electrical Conductivity, σ (S/m)			Thermal Conductivity, λ (W/m-K)			
a_n	B_nC	TiO_x	Cu[17]	B_nC	TiO_x	AlN	Cu[17]
a_0	+ 69,183.9814	+ 326,853.272	$+ 1.0390 \times 10^{9}$	$+ 11.3396707$	$+ 4.08237403$	+ 180	+ 1332.54048
a_1	− 1234.03868	− 4144.27626	$- 1.1656 \times 10^{7}$	$- 5.2304 \times 10^{-2}$	$- 8.1921 \times 10^{-3}$	0	− 10.6963322
a_2	+ 9.06460002	+ 23.2027347	+ 59,988.6377	$+ 3.5065 \times 10^{-4}$	$+ 1.9140 \times 10^{-5}$	0	$+ 5.1873 \times 10^{-2}$
a_3	$- 3.5326 \times 10^{-2}$	$- 6.9261 \times 10^{-2}$	− 174.038879	$- 1.2338 \times 10^{-6}$	$- 1.5209 \times 10^{-8}$	0	$- 1.4055 \times 10^{-4}$
a_4	$+ 8.0141 \times 10^{-5}$	$+ 1.2361 \times 10^{-4}$	+ 0.30654755	$+ 2.5075 \times 10^{-9}$	$+ 4.0526 \times 10^{-12}$	0	$+ 2.3203 \times 10^{-7}$
a_5	$- 1.0801 \times 10^{-7}$	$- 1.3668 \times 10^{-7}$	$- 3.3435 \times 10^{-4}$	$- 3.0343 \times 10^{-12}$	0	0	$- 2.3923 \times 10^{-10}$
a_6	$+ 8.5038 \times 10^{-11}$	$+ 9.1972 \times 10^{-11}$	$+ 2.2058 \times 10^{-7}$	$+ 2.1485 \times 10^{-15}$	0	0	$+ 1.5062 \times 10^{-13}$
a_7	$- 3.6120 \times 10^{-14}$	$- 3.4546 \times 10^{-14}$	$- 8.0640 \times 10^{-11}$	$- 8.1975 \times 10^{-19}$	0	0	$- 5.3013 \times 10^{-17}$
a_8	$+ 6.3958 \times 10^{-18}$	$+ 5.5573 \times 10^{-18}$	$+ 1.2538 \times 10^{-14}$	$+ 1.2986 \times 10^{-22}$	0	0	$+ 7.9972 \times 10^{-18}$

Table II. Polynomial constants for calculating the Seebeck coefficient for the applied thermoelectric materials

	Seebeck Coefficient, S (V/K)	
a_n, b_n	B_nC	TiO_x
a_0	$- 6.3272 \times 10^{8}$	$- 1.5079 \times 10^{9}$
a_1	$+ 1.0483 \times 10^{7}$	$+ 8.1327 \times 10^{6}$
a_2	− 19,130.6716	− 48,945.4351
a_3	+ 8.34824275	+ 113.495835
a_4	$- 3.6036 \times 10^{-3}$	$- 9.2332 \times 10^{-2}$
a_5	$+ 5.2797 \times 10^{-6}$	$+ 1.7401 \times 10^{-5}$
b_0	+ 1	+ 1
b_1	$+ 1.7299 \times 10^{10}$	$+ 1.0963 \times 10^{11}$
b_2	$+ 2.1244 \times 10^{7}$	$- 2.1360 \times 10^{8}$
b_3	− 126,576.761	− 30,245.2753
b_4	+ 91.7957010	+ 163.766515

Following Ref. [16], the heat flux can also be written as

$$\dot{Q}_1 = \frac{1}{R_{\text{teg}}}\left(T_1^* - T_2^*\right) - \frac{R_{\text{i}} I^2}{2} + m S_{\text{eff}} I T_1^*, \tag{7}$$

$$\dot{Q}_2 = \frac{1}{R_{\text{teg}}}\left(T_1^* - T_2^*\right) + \frac{R_{\text{i}} I^2}{2} + m S_{\text{eff}} I T_2^*, \tag{8}$$

with the matched internal electrical TEG resistance R_{i}, which yields for the current $I = m S_{\text{eff}}\left(T_1^* - T_2^*\right)/(2R_{\text{i}})$, where $S_{\text{eff}} = (S_{\text{BC}} - S_{\text{TiO}})$ is the effective Seebeck coefficient for one pair of thermoelectric legs. The internal electrical TEG resistance is defined as

$$R_{\text{i}} = m\left(\frac{\rho_{\text{TiO}} l_{\text{l}}}{A_{\text{l}}} + \frac{\rho_{\text{BC}} l_{\text{l}}}{A_{\text{l}}}\right). \tag{9}$$

In Eq. 9, ρ is the electrical resistivity, which is defined as the reciprocal of the electrical conductivity σ given in Table I. We aggregate Eqs. 5, 6, 7, 8, and 9 in matrix form $\underline{\underline{M}} \cdot \underline{x} = \underline{b}$

$$\begin{bmatrix} R_{\text{hx1}} & 1 & 0 & 0 & 0 & 0 \\ -1 & \frac{1}{R_{\text{con}}} & -\frac{1}{R_{\text{con}}} & 0 & 0 & 0 \\ -1 & 0 & \frac{1}{R_{\text{teg}}} + m S_{\text{eff}} I & -\frac{1}{R_{\text{teg}}} & 0 & 0 \\ 0 & 0 & \frac{1}{R_{\text{teg}}} & -\frac{1}{R_{\text{teg}}} + m S_{\text{eff}} I & 0 & -1 \\ 0 & 0 & 0 & \frac{1}{R_{\text{con}}} & -\frac{1}{R_{\text{con}}} & -1 \\ 0 & 0 & 0 & 0 & 1 & -R_{\text{hx2}} \end{bmatrix} \cdot \begin{pmatrix} \dot{Q}_1 \\ T_1 \\ T_1^* \\ T_2^* \\ T_2 \\ \dot{Q}_2 \end{pmatrix} = \begin{pmatrix} T_{\infty 1} \\ 0 \\ \frac{R_{\text{i}} I^2}{2} \\ -\frac{R_{\text{i}} I^2}{2} \\ 0 \\ T_{\infty 2} \end{pmatrix} \tag{10}$$

so that the sought values are calculated by $\underline{x} = \underline{\underline{M}}^{-1} \cdot \underline{b}$. As the hot-side temperature, as a

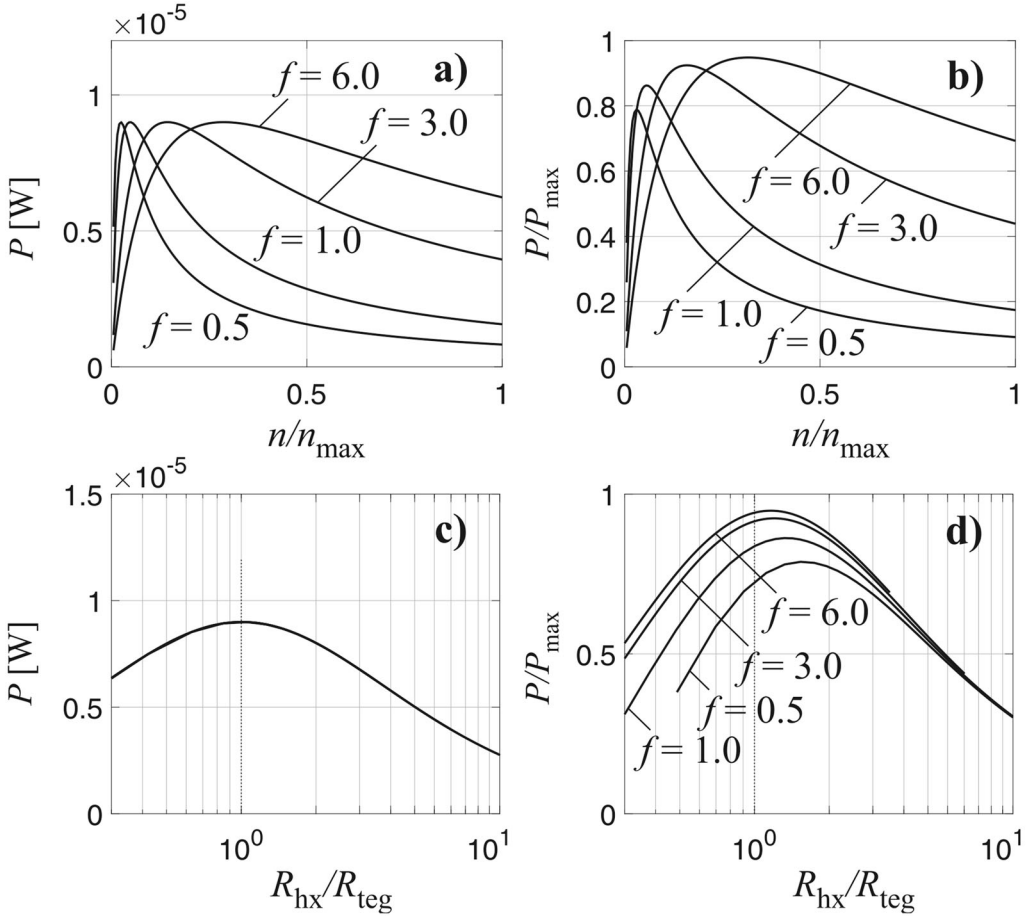

Fig. 2. Electrical power output versus leg number (a, b) and versus thermal resistance ratio (c, d) for various leg form factors in configuration A, when neglecting (a, c) or considering (b, d) parasitic heat losses.

boundary condition, is directly applied to the surface of the TEG, it follows that $R_{hx1} = 0$, yielding $T_{\infty 1} = T_1$. For the cold side, $R_{hx2} = R_{hx}$ applies, according to Eq. 4. The temperature-dependent material properties are determined at their individual mean temperature $\bar{T} = (T_{max} + T_{min})/2$, and with a guessed initial temperature condition, Eq. 10 is solved iteratively. Finally, the TEG output power is calculated by

$$P = \dot{Q}_1 - \dot{Q}_2 = mS_{eff}I\left(T_1^* - T_2^*\right) - R_iI^2. \qquad (11)$$

NUMERICAL RESULTS

Optimum Thermal Resistance Matching

The TEG–heat exchanger system will be analyzed once at a low hot-side temperature $T_{\infty 1}$ = 333.15 K with a small temperature gradient and once at a high hot-side temperature $T_{\infty 1}$ = 873.15 K with a large temperature gradient. The ambient cold-side temperature is held constant at $T_{\infty 2}$ = 323.15 K.

Configuration A: Optimum thermal resistance matching for hot-side temperature $T_{\infty 1}$ = 333.15 K.

Applying a temperature gradient of 10 K results in a rather small electrical power output with maximal performance of P_{max} = 9 × 10^{-6} W (Fig. 2-a). It is remarkable that the maximum power is the same for all chosen form factors f when neglecting the internal heat bypass ($R_{by,\lambda} = R_{by,\epsilon} = \infty$). To achieve this output power, specific leg numbers have to be applied. This behavior is caused by the variable temperature difference $\Delta T = T_1^* - T_2^*$ that depends on the thermal resistance of the thermoelectric module which, again, depends on the number of legs. For only a few leg pairs does the thermal resistance of the module as well as the difference in temperature ΔT rise, leading to high leg-specific power output. In contrast, the TEG module is characterized by low leg-specific power output for almost fully occupied modules, since its thermal resistance decreases remarkably. Between these two scenarios, the product of the leg number and the leg-specific power output achieves a global maximum. When considering parasitic heat losses, the maximum achievable power depends on the form factor f (Fig. 2b). Furthermore, the heat bypass leads to a decrease of the TEG performance. This effect is especially emphasized for short legs, as

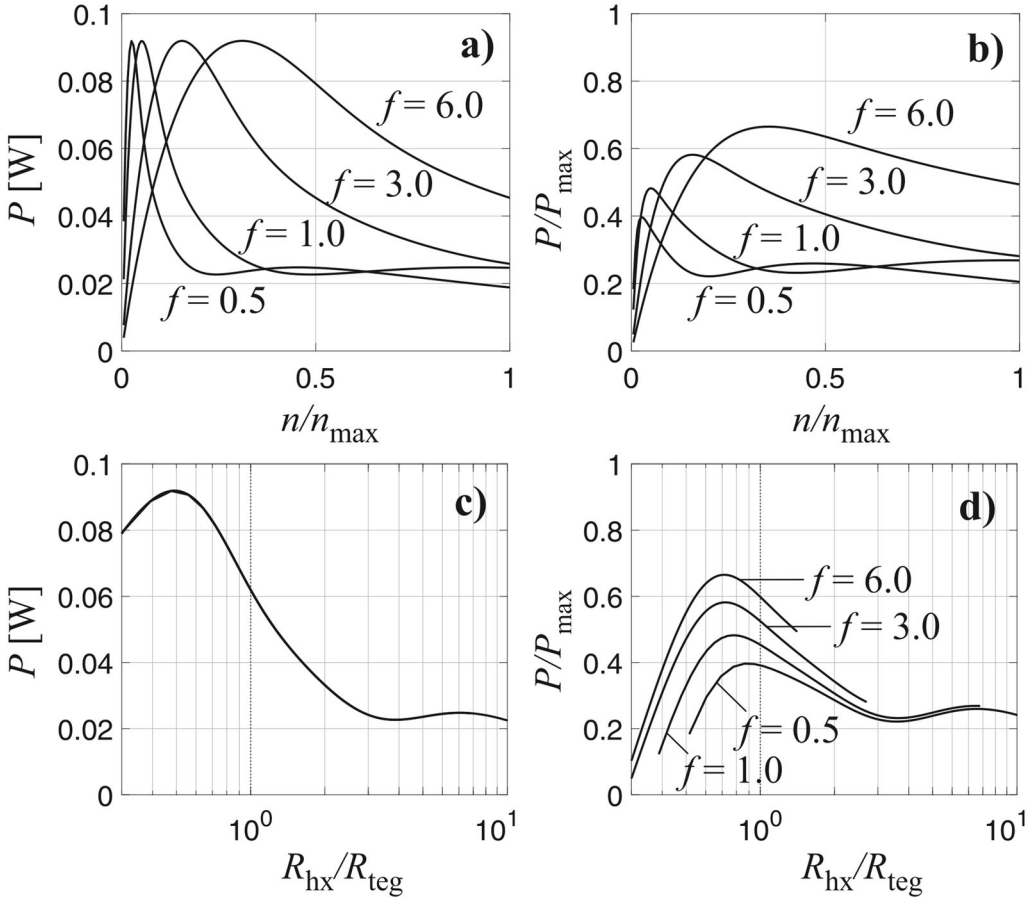

Fig. 3. Electrical power output versus leg number (a, b) and versus thermal resistance ratio (c, d) for various leg form factors in configuration B, when neglecting (a, c) or considering (b, d) parasitic heat losses.

the conductive resistance $R_{by,\lambda}$ is then comparatively small.

By calculating the power output as a function of the thermal resistance ratio, the conclusions of Henderson and Stevens[6,7] can be confirmed in case of neglecting thermal losses within the TEG. Under these conditions, the maximum power can be found at the thermal resistance ratio $R_{hx}/R_{teg} = 1$ and the performance does not depend on the chosen leg form factor (Fig. 2c). In contrast, inclusion of heat losses results in a shift in the optimum thermal resistance ratio (Fig. 2d). This shift is not constant but depends on the leg geometry, as this parameter influences the amount of heat transfer in the thermoelectric legs and in the space between them. The difference between the power curves in Fig. 2c and d can be seen as the main finding presented in this article, depicting the importance of considering parasitic heat losses in modeling TEG performance.

Configuration B: Optimum thermal resistance matching for hot-side temperature $T_{\infty 1}$ = 873.15 K.

The hot-side temperature applicable for the intended ceramic-based TEG should reach up to 600°C. When applying this boundary condition for the mathematical modeling, a large performance boost to $P_{max} = 9.2 \times 10^{-2}$ W can be observed (Fig. 3a). There are also two important differences in the TEG performance in comparison with configuration A. First, the heat loss due to radiation has increased because of the higher temperature range. This results in a stronger drop in the maximum performance and reaches merely almost 70% for leg form factor f = 6.0 and less than 40% in case of f = 0.5 (Fig. 3b). Secondly, when neglecting the heat losses, the optimum thermal resistance ratio is again independent of the form factor f, but a constant shift occurs (Fig. 3c). This shift is caused by the temperature-dependent material parameters, yielding a variable figure of merit ZT for the examined TEG. Additionally, that effect causes the formation of a local maximum at $R_{hx}/R_{teg} \approx 8$. The shift in the matched thermal resistance ratio due to the temperature-dependent material parameters and due to the internal heat loss overlaps as seen in Fig. 3d.

Multiobjective Module Design Optimization

In the previous section, the focus was on maximization of the total TEG power output. Besides the performance, there are sometimes other parameters which have to be optimized in a proper module

design; For example, product costs should be as low as possible. Especially when novel high-grade thermoelectric substances are applied, material costs can make a significant contribution to the total cost of a thermoelectric module. In this case, a further objective arises, viz. maximization of the total power output with regard to the total built-in amount of thermoelectric material, which can be measured by the volume $V_l = nA_l l_l$. The lower the amount of material needed to reach the power output, the less expensive the module. In other cases, the amount of exploitable heat may be limited, so that the efficiency of the thermoelectric system becomes more important. Then, guaranteeing the best efficiency constitutes another objective.

When a TEG module must be designed to maximize more than one parameter, special mathematical techniques for multiobjective optimization have to be applied. A visual approach to solve that issue is given by identifying optimal design variants with the help of generated Pareto frontiers. For this purpose, the quantity of a first objective is plotted against the quantity of a second objective for all possible module variants. Designs are Pareto efficient when there is no other configuration that maximizes one of the objectives without reducing the other. When aggregating all design variants into one diagram, the Pareto frontier is, therefore, formed by the set of allocations at the upper-right boundary of the solution area.

Such analysis was done for a set of TEG modules with 1000 randomly chosen form factors f by applying the thermal boundary conditions of configuration B ($T_{\infty 1}$ = 873.15 K, $T_{\infty 2}$ = 333.15 K). For each form factor, the module performance was calculated considering all possible leg pair numbers from m = 1 to fully occupied variants with m = 200. The multiobjective optimization was then carried out for the total power output against the reciprocal of the built-in volume of thermoelectric material (Fig. 4). The solutions for all leg number configurations for modules with form factors of f = 0.5, 1.0, 3.0, and 6.0 are highlighted exemplarily. The enlargement in Fig. 4 demonstrates that applying the optimum leg number that yields the maximum power output is not a Pareto-efficient design. Here, the maximum power point is analyzed for a module with f = 1.0 (design variant ①: f = 1.0, n = 20, V_l = 540 mm^3, P = 44.36 mW). This allocation is clearly not part of the Pareto frontier, meaning that the total power output can be increased by 0.56% with no requirement for more thermoelectric material (design variant ②: f = 1.1095, n = 18, V_l = 539.2 mm^3, P = 44.61 mW). Additionally, the power output of design ① can be reached with 6.63% less thermoelectric materials when choosing a

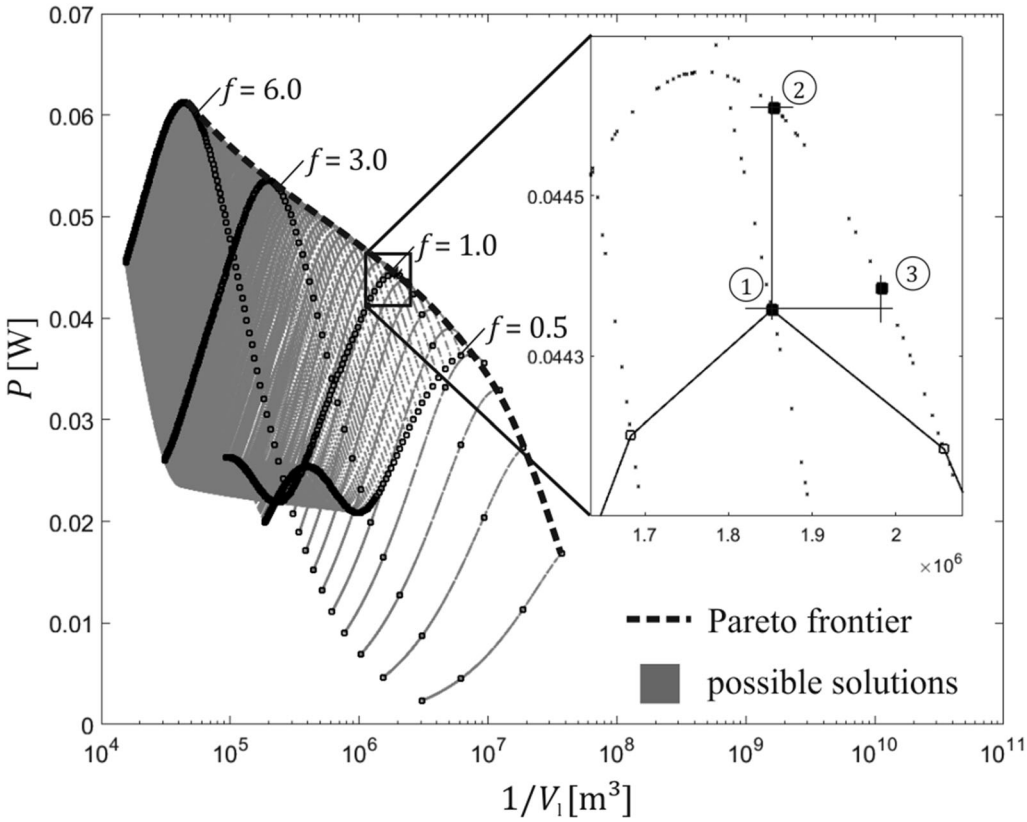

Fig. 4. Electrical power output versus built-in amount of thermoelectric material for 1000 randomly chosen leg form factors. Results for form factor f = 0.5, 1.0, 3.0, and 6.0 are exemplary highlighted. The enlargement compares the best-performing design regarding the form factor f = 1.0 with Pareto-efficient design variants.

Pareto-efficient design instead (design variant ③: $f = 1.0373$, $n = 18$, $V_l = 504.15\ \text{mm}^3$, $P = 44.38$ mW).

CONCLUSIONS

Possibilities to optimize the design of a TEG–heat exchanger system are investigated. For given heat exchanger properties, it is shown that a certain built-in leg number maximizes the performance of the entire thermoelectric system. To identify the optimum leg number, a mathematical model based on a thermal resistance network was implemented.

The aims of this work were to prove the findings of Henderson[6] and Stevens[7] for high-temperature applications of thermoelectric systems and to develop a design strategy for versatile TEG modules applicable in high temperature ranges. In case of low temperatures and negligible heat losses, the proposed optimum thermal resistance ratio R_{hx}/R_{teg} can be confirmed to be approximately equal to 1. Based on this behavior, the design strategy can be simplified to the following three steps:

1. Construct proper thermal connection. The better the heat exchanger performance, the more energy can be harvested. Sufficient heat transfer rates can be easily achieved using methods of forced convection. However, for such active TEG cooling and heating techniques, auxiliary power to drive fans or pumps is necessary, decreasing the net electrical output. Therefore, passive heat transfer concepts utilizing natural convection are rather favored.
2. Characterize the heat exchangers by their thermal resistances. The sum of all external thermal resistances is of interest. Additionally, thermal contact resistances have to be taken into account.
3. TEG module assembly according to optimum thermal resistance ratio. In the present study, it is shown that the thermal resistance of the modules can be adapted by adjusting the number of legs while keeping other design parameters constant. Regarding the manufacturing of the TEG, this approach is time and cost saving, since the tool for producing the thermoelectric legs can be applied even for different module designs.

Especially for the application of the examined TEG model at high temperatures, a remarkable shift in the optimum thermal resistance ratio can be observed. This shift is caused by the temperature-dependent material parameters as well as the internal parasitic heat losses. This shift depends on the applied temperature and the chosen leg geometry, which makes the proposed design strategy more complex. Instead of defining a constant thermal resistance for the TEG module, individual leg numbers for each given boundary condition have to be determined. Therefore, proper theoretical models supported by experimental investigation to measure, for instance, the effect of thermal contact resistances are necessary.

With the proposed thermal resistance network, the leg number was adjusted, on the one hand, to maximize the electrical power output and, on the other hand, to optimize the TEG module design regarding multiple objectives simultaneously. In case of the latter task, the electrical power output was optimized versus the amount of built-in thermoelectric material. Here, some fine-tuning opportunities were revealed. For an examined example, it was shown that the total power output can be increased by 0.56% with no requirement for more thermoelectric material. In turn, it was also demonstrated for this example that the demand for thermoelectric material can be reduced by 6.63% without electrical power losses.

ACKNOWLEDGMENTS

The authors are grateful for financial support from Sächsische AufbauBank (Grant No. 100234924). Furthermore, the authors would like to thank Fraunhofer Institute for Ceramic Technologies and Systems (IKTS) and the Chair of Hydrogen and Nuclear Energy (WKET) for providing material data as well as productive discussions.

REFERENCES

1. L. Mateu, C. Codrea, N. Lucas, M. Pollak, and P. Spies, in *Proceedings of XXI Conference on Design of Circuits and Integrated Systems. DCIS* (2006), pp. 22–24.
2. M. Tewolde, C. C. Lin, H. Tao, H. Chen, G. Fu, D. Liu, T. Zhang, D. Benjamin, L. Zuo, D. Hwang, and J. Longtin, in *Proceedings of the ASME* (2014).
3. J. Chen, L. Zuo, Y. Wu, and J. Klein, *Energy Convers. Manag.* 122, 298 (2016).
4. M. Hauck and M. S. Ward, US9263659B2 (2016).
5. T. Zhu, Y. Liu, C. Fu, J.P. Heremans, J.G. Snyder, and X. Zhao, *Adv. Mater.* 29, 1605884 (2017).
6. J. Henderson, in *Proceedings of the 14th Intersociety Energy Conversion Engineering Conference* (1979), pp. 1835–1840.
7. J.W. Stevens, *Energy Convers. Manag.* 42, 709 (2001).
8. Y. Apertet, H. Ouerdane, O. Glavatskaya, C. Goupil, and P. Lecoeur, *EPL Europhys. Lett.* 97, 28001 (2012).
9. H. Xiao, X. Gou, and S. Yang, *J. Electron. Mater.* 40, 1195 (2011).
10. Z.-G. Shen, S.-Y. Wu, L. Xiao, and G. Yin, *Energy* 95, 367 (2016).
11. R. Bjørk, D.V. Christensen, D. Eriksen, and N. Pryds, *Int. J. Therm. Sci.* 85, 12 (2014).
12. P. Ziolkowski, P. Poinas, J. Leszczynski, G. Karpinski, and E. Müller, *J. Electron. Mater.* 39, 1934 (2010).
13. M. Barry, J. Ying, M.J. Durka, C.E. Clifford, B.V.K. Reddy, and M.K. Chyu, *Energy* 102, 427 (2016).
14. VDI, *Wärmeatlas: Berechnungsblätter für den Wärmeübergang*, 9th ed. (Heidelberg: Springer, 2002).
15. H.D. Baehr and K. Stephan, *Wärme- und Stoffübertragung*, 8th ed. (Heidelberg: Springer, 2013).

16. A.F. Ioffe, *Semiconductor Thermoelements and Thermoelectric Cooling* (London: Infosearch, 1957).
17. Deutsches Kupferinstitut, Werkstoff-Datenblätter Cu-ETP (2005).